

Multi-Angle Imager for Aerosols Thermal Control System

Douglas A. Bolton¹ and Rogelio Rosas²

Jet Propulsion Laboratory, California Institute of Technology, Pasadena, California, 91109

The Multi-Angle Imager for Aerosols (MAIA) Thermal Control System is a NASA funded instrument that will collect data to help characterize airborne particulate matter over a number of population centers across the globe using multi-angle spectropolarimetric imagery. The data collected by MAIA will facilitate assessments of the impacts of different types of particulate matter on adverse health outcomes. MAIA is a hosted payload meant to operate in a near-circular sun-synchronous polar orbit, with a mean altitude between 600 km and 850 km. The nominal on-orbit mission design lifetime is three years. Temperature control of the MAIA instrument is accomplished with a combination of passive radiators and heaters. The focal plane module (FPM) is cooled to $\leq 235\text{K}$ with a disc shaped radiator that faces the anti-sun side of the sun-synchronous orbit. The temperature of the MAIA cameras and associated electronics is controlled with a cylindrical shaped radiator that projects a near constant area in the nadir direction as the cameras rotate. A noteworthy feature of the MAIA thermal control system design is the novel, low cost, rotationally articulating thermal strap used to transfer heat from the FPMs to their associated FPM Radiator. The strap spans one of the axes of rotation, sweeping out an arc of approximately 60° as the instrument operates. A prototype of the articulating thermal strap was life tested to 260,000 cycles with no signs of significant degradation. An overview of the MAIA thermal control system baseline design is presented, with focus on its novel aspects, including life testing of the prototype articulating thermal strap. In addition, a discussion of the considerations involved in designing a thermal control system for a hosted instrument is provided.

Nomenclature

<i>APG</i>	=	<i>Annealed Pyrolytic Graphite</i>
<i>DEU</i>	=	<i>Drive Electronics Unit</i>
<i>FOR</i>	=	<i>Field Of Regard</i>
<i>FOV</i>	=	<i>Field Of View</i>
<i>FPA</i>	=	<i>Focal Plane Array</i>
<i>FPM</i>	=	<i>Focal Plane Module</i>
<i>LEO</i>	=	<i>Low Earth Orbit</i>
<i>MAIA</i>	=	<i>Multi-Angle Imager for Aerosols</i>
<i>MLI</i>	=	<i>Multi-Layer Insulation</i>
<i>NPR</i>	=	<i>NASA Procedural Requirement</i>
<i>OBC</i>	=	<i>On Board Calibrator</i>
<i>PM</i>	=	<i>Particulate Matter</i>
<i>SALMON</i>	=	<i>Stand-Alone Mission of Opportunity</i>
<i>SLI</i>	=	<i>Single-Layer Insulation</i>
<i>VDA</i>	=	<i>Vapor Deposited Aluminum</i>

¹ Technical Group Lead, Cryogenic Systems Engineering, 4800 Oak Grove Drive, Pasadena, CA 91109-8099, M/S 157-316.

² Thermal Engineer, Cryogenic Systems Engineering, 4800 Oak Grove Drive, Pasadena, CA 91109-8099, M/S 157-316.

Copyright © 2018 California Institute of Technology, Government sponsorship acknowledged.

The decision to implement MAIA will not be finalized until NASA's completion of the National Environment Policy Act (NEPA) process. This document is being made available for information purposes only.

I. Introduction

The MAIA instrument was selected as a Stand-Alone Mission of Opportunity (SALMON) in March of 2016. The instrument is classified as Category 3 per NASA Procedural Requirement (NPR) 7120.5E and Class C per NPR 8705.4. Primary project activities are taking place at the Jet Propulsion Laboratory, California Institute of Technology, in Pasadena, CA.

The MAIA project is designed to assess the impacts of different size and compositional mixtures of airborne particulate matter (PM) on adverse human health outcomes¹. This is accomplished by collecting multi-angle spectropolarimetric imagery over targets of interest, as shown in Figure 1. As illustrated in Figure 2, targets of interest include major population centers on 5 continents¹. Each target of interest will be observed at least 3 times per week on average over the 3 year life of the mission¹. The MAIA instrument budget is cost capped at \$97 million in fiscal 2018 dollars¹.

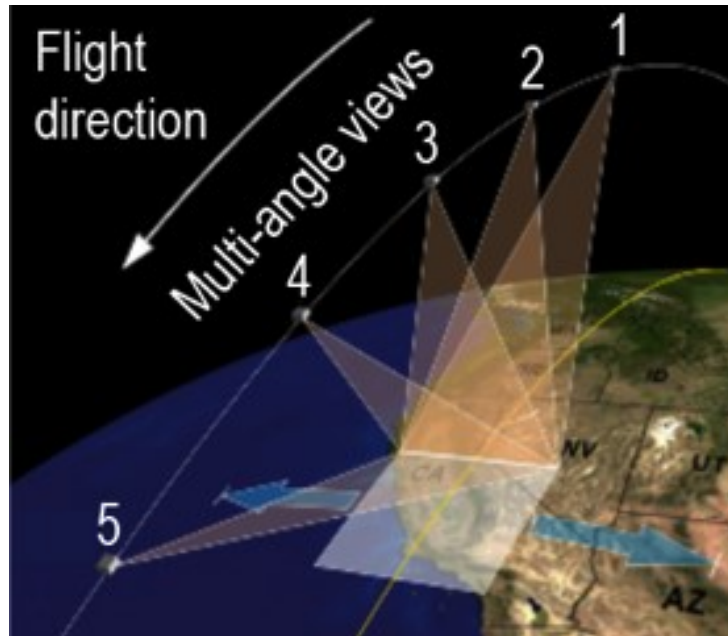


Figure 1. MAIA Multi-Angle Imaging Approach.



Figure 2. MAIA Regions of Interest.

II. Instrument Description

The MAIA instrument measures the characteristics of sunlight scattered by atmospheric aerosols. This information is used to determine the type and quantity of PM in near-ground level atmosphere where human health is likely to be influenced. The MAIA instrument flies in a sun-synchronous low earth orbit (LEO) and utilizes spectropolarimetric cameras on a two-axis gimbal system for multi-angle viewing. The first rotational axis moves the cameras in an along-track or “Scan” direction to positions directly below the orbital path. The second axis rotates the cameras in a cross-track or “Pan” direction to point the cameras to locations on either side of the orbital path, as shown in Figure 3. The Scan axis rotation provides a field of regard (FOR) of $\pm 60^\circ$ in the along-track direction with the Pan Axis rotation providing a $\pm 45^\circ$ cross-track FOR.

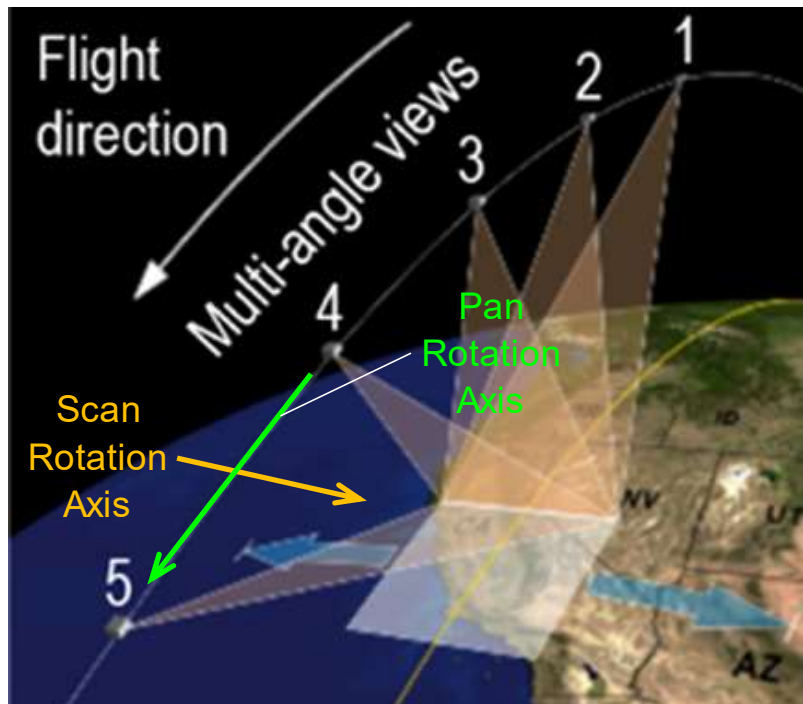


Figure 3. MAIA Rotational Axes Relative to Orbit Direction.

Figure 4 provides an overall view of the major components on the exterior of the instrument. The Focal Plan Module (FPM) Radiator is on the $-Y$ side of the instrument. During operations, the $-Y$ axis of the instrument points towards the anti-sun side of the sun-synchronous orbit to minimize solar loading on the FPM Radiator. An earth shield is used to reduce the amount of earth emitted infrared spectrum energy incident on the FPM Radiator.

The $+Z$ axis of the instrument is pointed in the nadir direction to facilitate imaging. The on board calibrator (OBC) includes both illuminated and dark targets, and is used to calibrate the instrument periodically during operations. Stray light shields are used to prevent unwanted illumination of the camera baffles, and a debris shield is used to provide line-of-sight debris protection for the cameras while in the launch configuration.

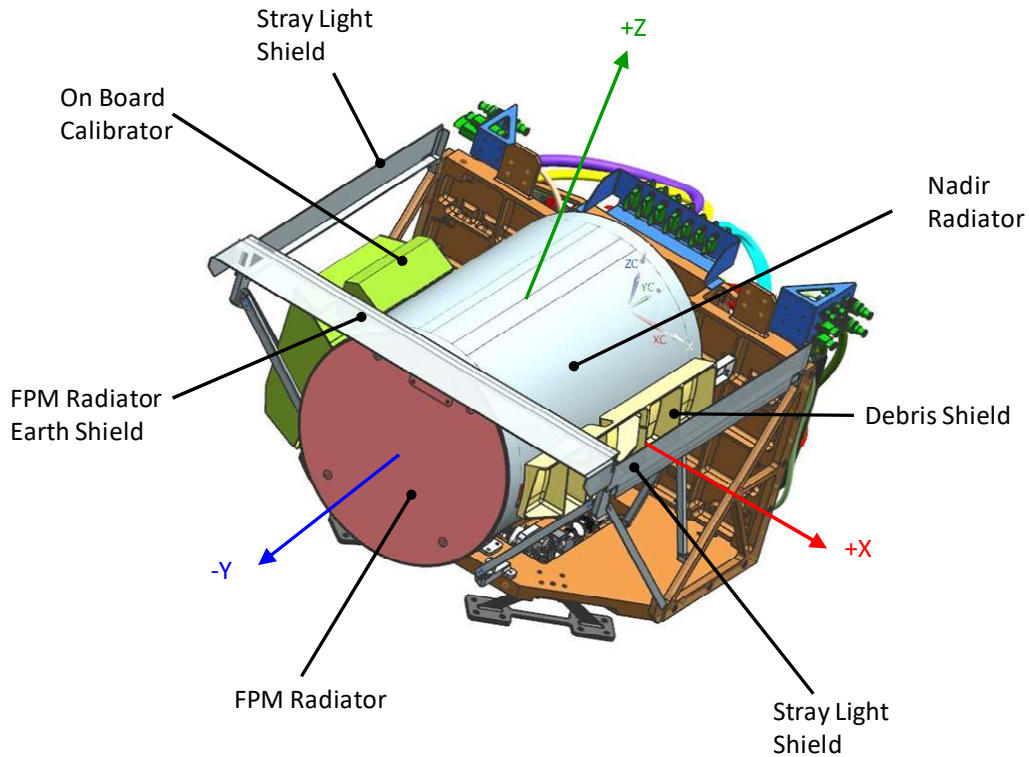


Figure 4. MAIA Instrument External Components.

Instrument internals are shown in Figures 5 and 6. The two cameras and their associated focal plane modules image across a wide range of spectral bands spanning wavelengths from 367 nm to 2126 nm. Imaging across this range of wavelengths requires the focal plane modules be cooled below 235K. Heat from the focal plane modules is transferred conductively across the Pan rotation axis using a rotationally articulating thermal strap. Note that the center of curvature of the strap is located on the Pan rotation axis. Highly conductive rigid thermal links are used to couple the ends of the articulating thermal strap to the FPM Radiator on one end, and FPM thermal straps on the other end.

Figures 5 and 6 also show the Scan and Pan rotation axes of the instrument. Note that both the FPM and Nadir radiators rotate together about the Scan axis. The cameras rotate about the Pan axis inside the Nadir Radiator. Scan and Pan gimbal mechanisms rotate $\pm 58^\circ$ and $\pm 30^\circ$ respectively to provide the $\pm 60^\circ$ and $\pm 45^\circ$ FORs about the +Z instrument axis. The Nadir Radiator projects a near constant area in the nadir direction as it rotates about the Scan axis. The gimbal arm shown in Figure 6 provides a coupling for the Pan and Scan gimbal mechanisms.

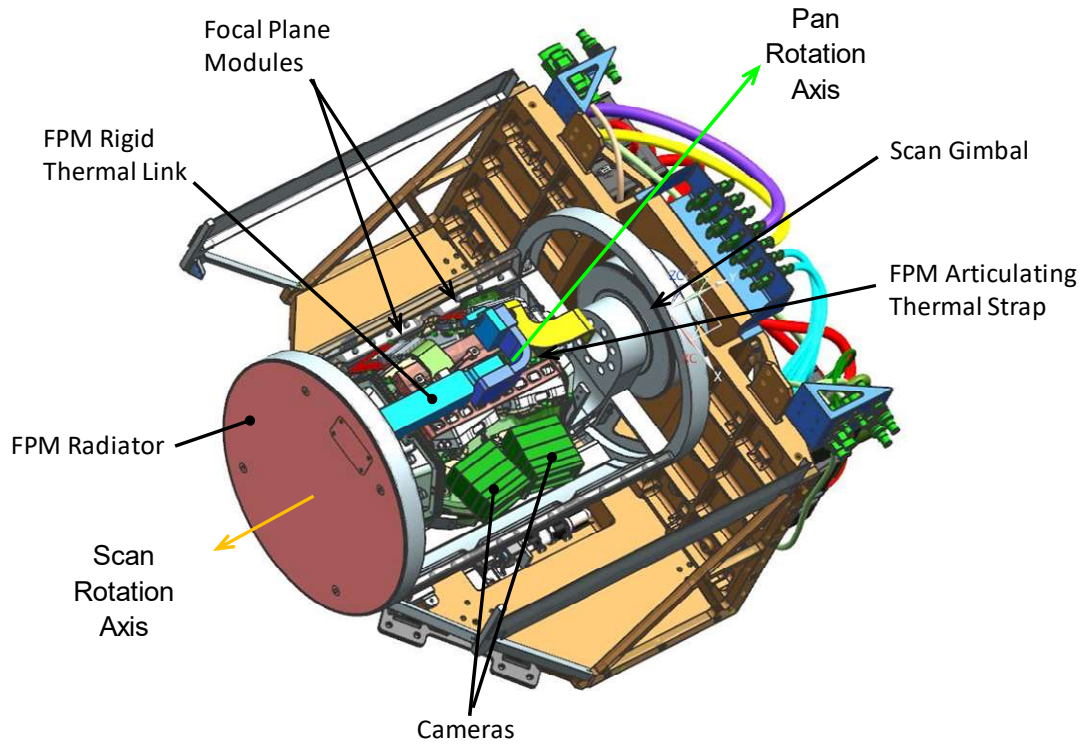


Figure 5. MAIA Instrument Internal Components, 1.

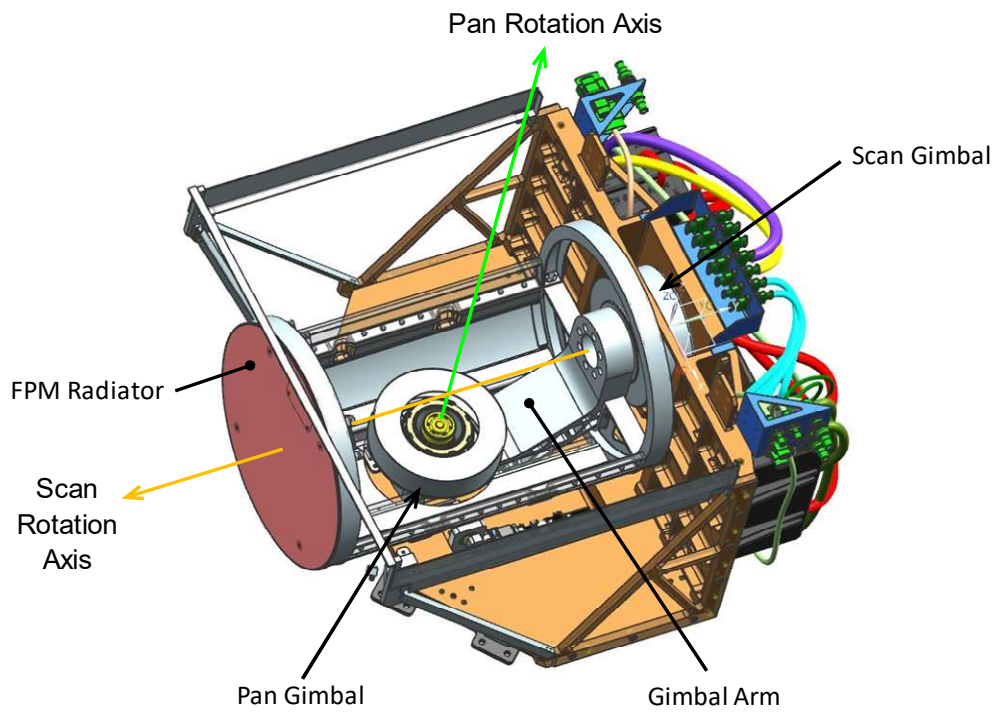


Figure 6. MAIA Instrument Internal Components, 2.

Data gathering, and instrument control functions are provided by the Instrument Electronics unit shown in Figure 7. The Instrument Electronics unit is mounted to the Gimbal Support Panel, the same structure that mounts the Scan Gimbal. Power and control for the Scan and Pan gimbal mechanisms is provided by the Drive Electronics Unit (DEU) which is also mounted to the gimbal support panel.

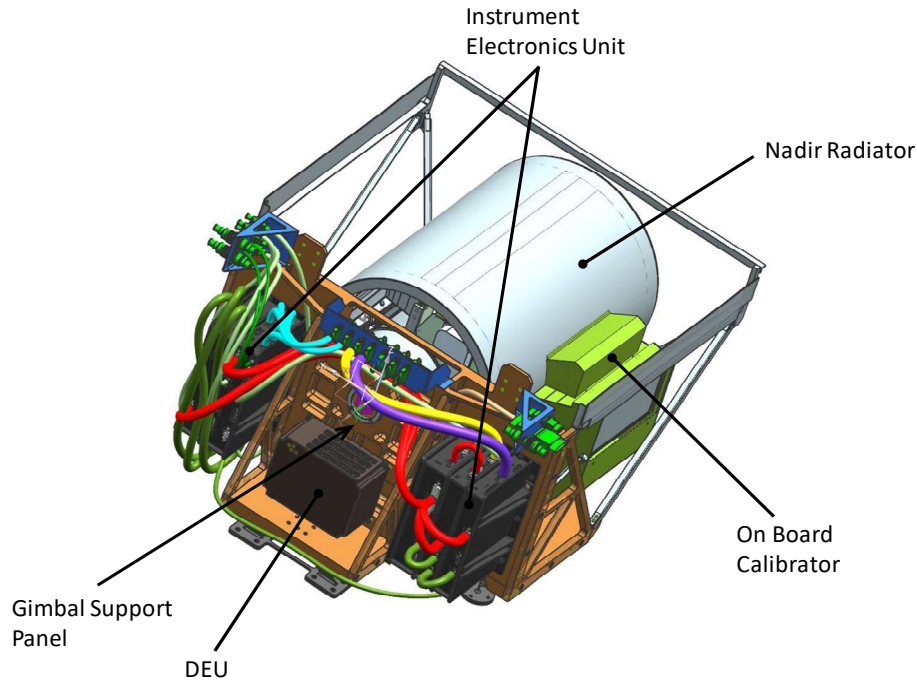


Figure 7. MAIA Instrument Electronics and DEU.

III. Thermal Environment

The MAIA instrument's mission will take place in a sun-synchronous near-polar orbit with an inclination of approximately 98° and an altitude between 600km and 850km². Orbital equator crossing times span from 9:00 am to 3:00 pm with an 11:30 am to 12:30 pm stay out zone². Solar beta angles will range from about 1° in an 11:30 am equator crossing orbit to 50° in a 3:00 pm equator crossing orbit.

IV. Notable Thermal Design Requirements

Key thermal requirements include controlling the focal plane array (FPA) temperatures to between 195K and 235K during imaging and maintain camera temperature between 283K and 308K. In addition, the FPAs must be controlled to a temperature stability of $\pm 0.1K$ and the cameras to $\pm 0.5K$ during target imaging.

V. Instrument Thermal Control System

Heat generated by the MAIA instrument is rejected to space by three main radiating surfaces, as shown in Figure 8. The FPM radiator faces the anti-sun side of the sun-synchronous orbit, providing a very stable sink for FPM heat rejection and temperature control. The cameras and camera electronics are conductively coupled to the camera platform through controlled conductance mounts. Heat from the camera platform radiates to the internal surface of the Nadir Radiator. The high emissivity external surfaces of the camera electronics units help to radiate their heat to the inside of the Nadir Radiator. The Nadir Radiator rejects waste heat from the cameras and camera electronics as it faces the earth during operations. The Gimbal Support Panel, shown in Figure 7, rejects excess heat from the Instrument Electronics and DEU. The Gimbal Support Panel has views to space on both the sun-facing and anti-sun

facing sides of the orbit. Note that all three of the main radiating surfaces utilize heaters to maintain temperatures and temperature stability within applicable limits.

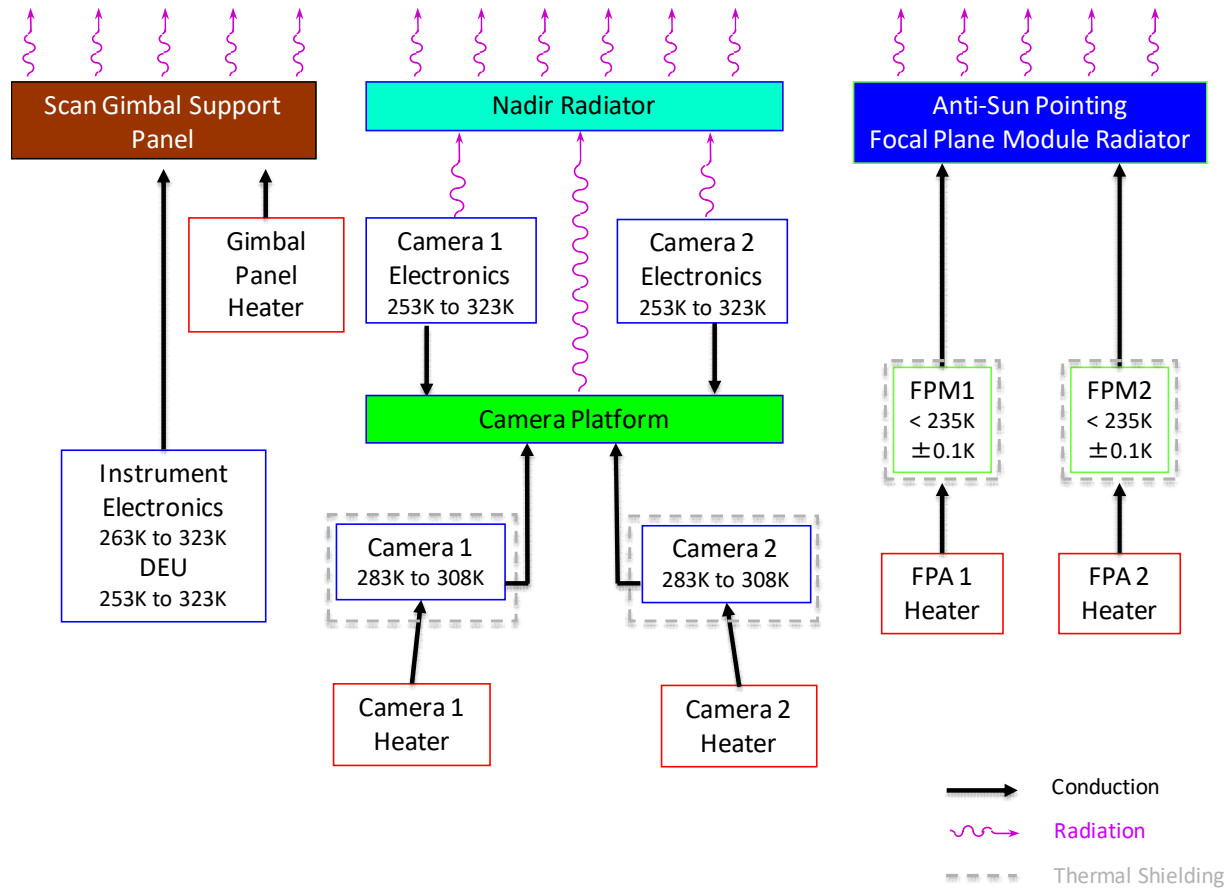


Figure 8. MAIA Thermal Control System Architecture.

The hardware involved in rejecting heat from the FPMs is shown in Figure 9. Heat from each camera FPM is conducted through a dedicated FPM thermal strap to a common T-shaped rigid thermal link. This thermal link interfaces with the moving end of the articulating thermal strap. The articulating thermal strap is made from 400 layers of 0.001 inch thick aluminum 1100 foil to maximize its flexibility. A second rigid thermal link spans the distance between the stationary end of the articulating thermal strap and the FPM radiator. Both rigid thermal links are made from aluminum encased Annealed Pyrolytic Graphite (APG). The FPM radiator is also made from aluminum encased APG encased in aluminum to improve in-plane conductance and maximize fin efficiency. The external surface of the FPM radiator is painted with S-13 white paint, and its internal surface is covered with multi-layer insulation (MLI). Both of the FPM thermal straps, the articulating thermal strap, and both rigid thermal links are covered with vapor deposited aluminum (VDA) coated Kapton, single-layer insulation (SLI). Not shown in Figure 9 are heaters and temperature sensors on the FPM thermal strap ends, and on the camera bodies. The heaters and temperature sensors provide temperature control for the FPMs and cameras.

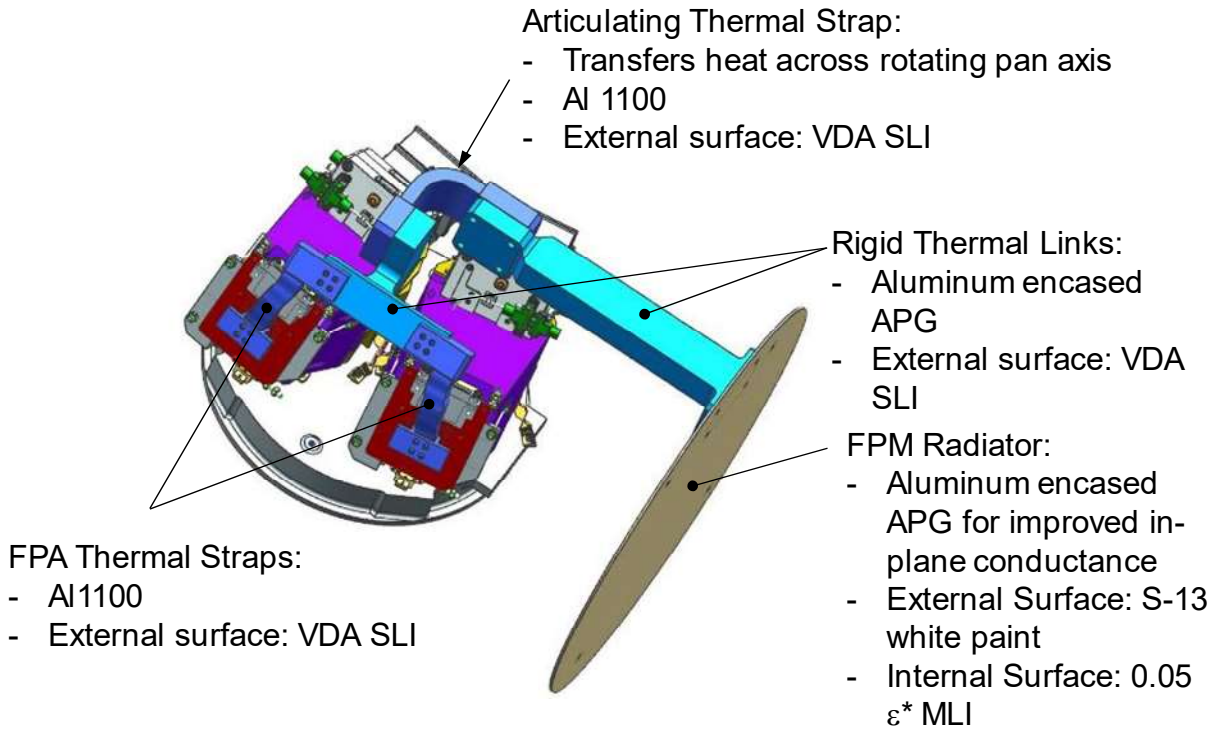


Figure 9. Focal Plane Module Temperature Control.

The Nadir Radiator is coated with S-13 white paint on its external surface and Z306 black paint on its internal surface (Figure 10). As mentioned earlier, heat from the cameras and camera electronics units is conducted through controlled conductance mounts to the camera platform. Both cameras are isolated radiatively with a single layer of VDA SLI on their external surfaces. The Z306 black paint coating on the camera platform helps the platform to reject heat radiatively to the inside of the Nadir Radiator. External surfaces of the camera electronics units are also coated with Z306 black paint to enhance radiative heat transfer to the nadir radiator.

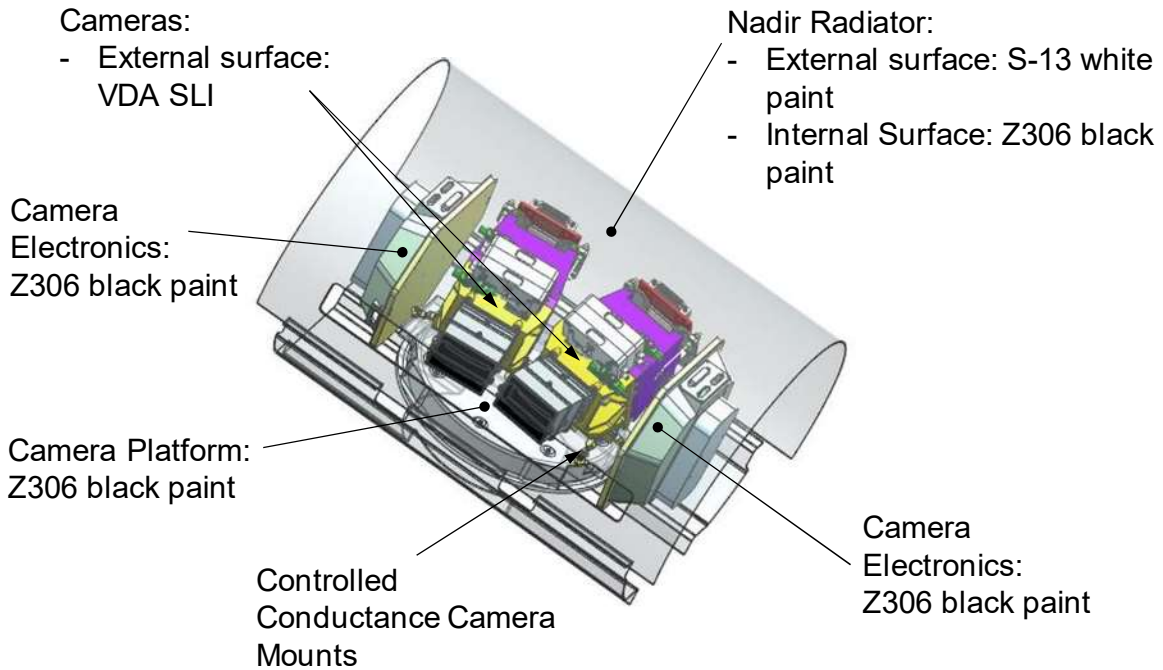


Figure 10. Camera Temperature Control.

Waste heat from the Instrument Electronics and DEU are conducted to the Gimbal Support Panel, Figure 11. The Gimbal Support Panel is painted with S-13 white paint on both sides. This coating helps the Gimbal Support Panel to radiatively reject the heat under the full range of expected environmental conditions. Not shown in Figure 11 is MLI insulation that will cover the harness and cables interfacing with the Instrument Electronics and DEU. Additional MLI will cover the Instrument Electronics and DEU units.

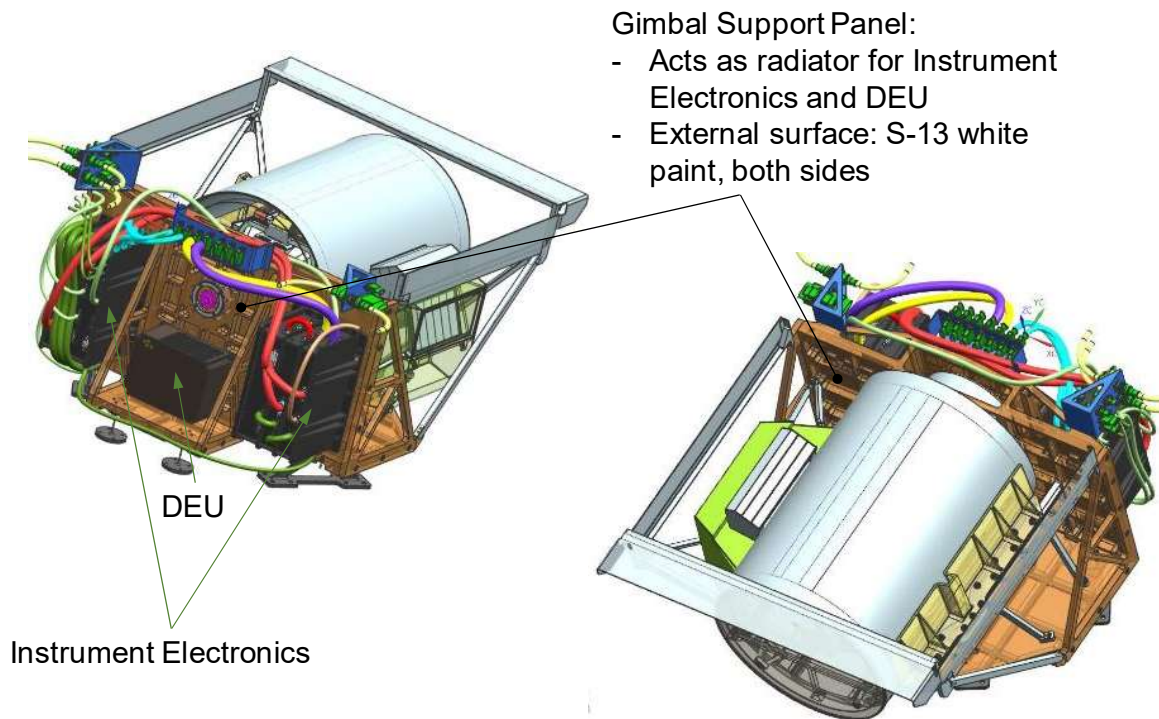


Figure 11. Instrument Electronics and DEU Temperature Control.

Expected unit dissipations are listed in Table 1. Note that each camera electronics unit will be dissipating a maximum of 9.36 watts, with the Pan gimbal actuator dissipation as high as 21.8 watts. This significant heat load inside the Nadir Radiator is one of the parameters that dictate its large surface area.

Table 1. Unit Dissipations.

Unit	Maximum Expected Dissipation (Per Unit, W)	Orbital Avg. Dissipation (Per Unit, W)
Camera Electronics	9.36	9.36
Camera (Modulator & Probe)	0.42	0.42
DEU	3.64	3.64
FPM Dissipation	0.295	0.295
Instrument Electronics	27.6	27.6
Pan Gimbal Actuator	21.8	3.43
Scan Gimbal Actuator	21.8	3.43

VI. Articulating Thermal Strap Life Testing

The MAIA instrument utilizes gimbal mechanisms that facilitate multi-angle viewing of selected target areas. The gimbal mechanisms provide for a field-of-regard of $\pm 60^\circ$ along-track and $\pm 45^\circ$ cross-track (about the +Z instrument axis). A rotationally articulating thermal strap is used to couple the MAIA FPAs to their radiator, while simultaneously allowing for gimbal movement. This special requirement could have been satisfied with a variety of solutions with a wide range of costs, but ultimately it was decided to utilize a simple aluminum thermal strap that was manufactured for compatibility with the planned gimbal movement angles. Due to the limited literature on the mechanical behavior of such an articulating strap, it was decided to conduct risk-reduction testing by subjecting a prototype strap to a life test utilizing an in-house built testing machine.

A. Rotationally Articulating Thermal Strap

The prototype strap was built in-house utilizing strips of 0.001 inch thick alloy 1100 aluminum foil that were approximately 8 inches long and 2 inches wide. The strap was stacked with 400 foil strips in order to match the proposed flight strap thickness of 0.4 inches. A jig was created to clamp the mounting brackets and strap ends together in order for the mounting hole pattern to be match drilled through all layers simultaneously. Figure 12 shows how these parts were assembled.

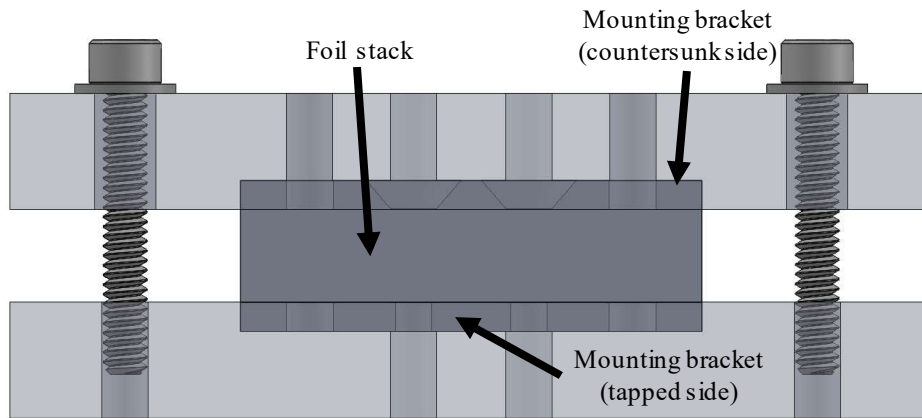
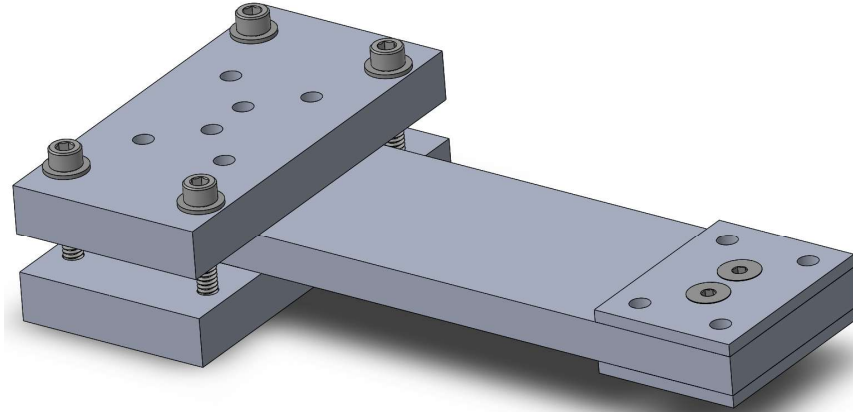


Figure 12. Strap Jig with Straight Aluminum Strap (top) and Cross-Section of Assembly (bottom).

The key to building a strap for this project was to build-in an appropriate curvature so that the desired range of motion could be accommodated without creating undo stress in any of the strap's layers. A strap built straight would create a tensile stress in layers at the larger bend radii when the strap is deformed, possibly resulting in tearing. As such, the prototype strap was formed at its minimum bend angle with longer layers at the outer bend radii and shorter layers at the inner bend radii. This creates a stress-free condition at the minimum strap bend angle, and puts the outer strap layers in compression at the maximum bend angle.

The strap was manufactured by using special built tooling to fix it to the curvature it would assume at its minimum bend angle. The foil stack was then locked-in by tightening down the bolts at the corners of the jig. Tightening these bolts prevented the strap from springing back to its flat position. The assembly was then put into a mill where the hole pattern was drilled. Figure 13 shows the completed prototype strap that was used for testing.

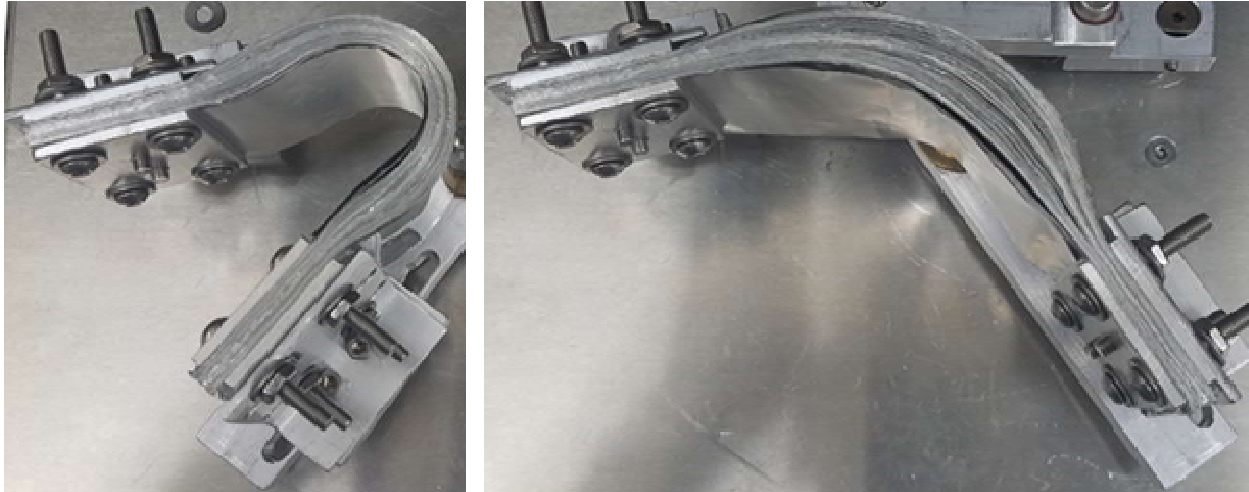


Figure 13. Prototype Strap Used for Risk-Reduction Testing at Minimum and Maximum Bend Angles.

B. Strap Cycle Machine

In order to cycle the articulating strap, a machine with an electric motor and a three-rod linkage system was devised. The main driving parameter for this machine was the $\pm 30^\circ$ across-track rotation needed to simulate the Pan gimbal movement. The machine was constructed to produce $\pm 35^\circ$ to ensure that the actual motion was bounded with margin. The two mounting points for the strap included the moveable end that was attached to the motor linkages and the fixed end that was stationary. The linkages were machined out of readily available 1"x1/2" aluminum bar stock and lengths were chosen based on the location of the motor and the need to conform to the expected range of rotation. The assembly was made out of aluminum into a compact, portable unit that encompassed a volume of about 12"x12"x13". Strap interface brackets were made with slotted holes for easy installation and adjustment of the articulating strap. A Bodine 33A series model 6037 motor was used to drive the system. Motor speed was controlled with a basic, off-the-shelf, Bodine speed controller. Figure 14 shows a top-down view of the unit, along with the angles of rotation that the main shaft follows. An isometric CAD view of the assembly is shown in Figure 15.

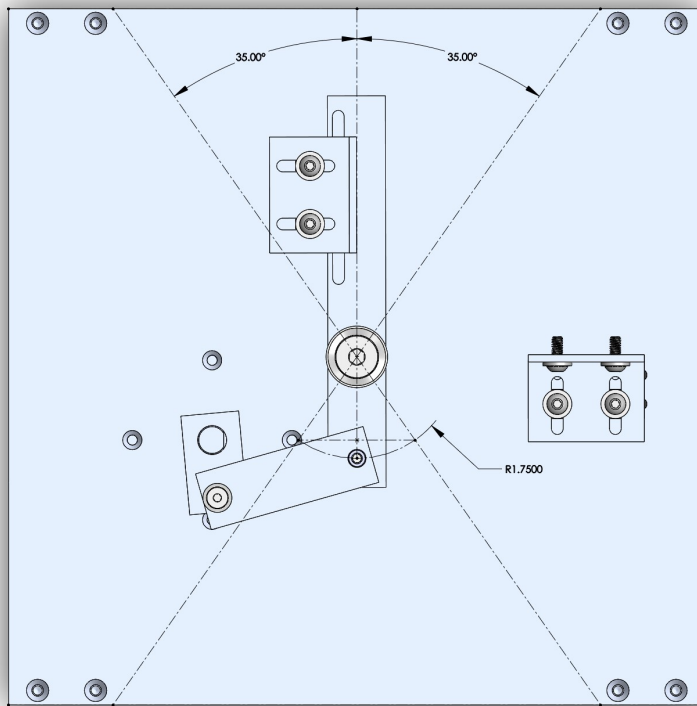


Figure 14. Top-View of Strap Cycle Machine.

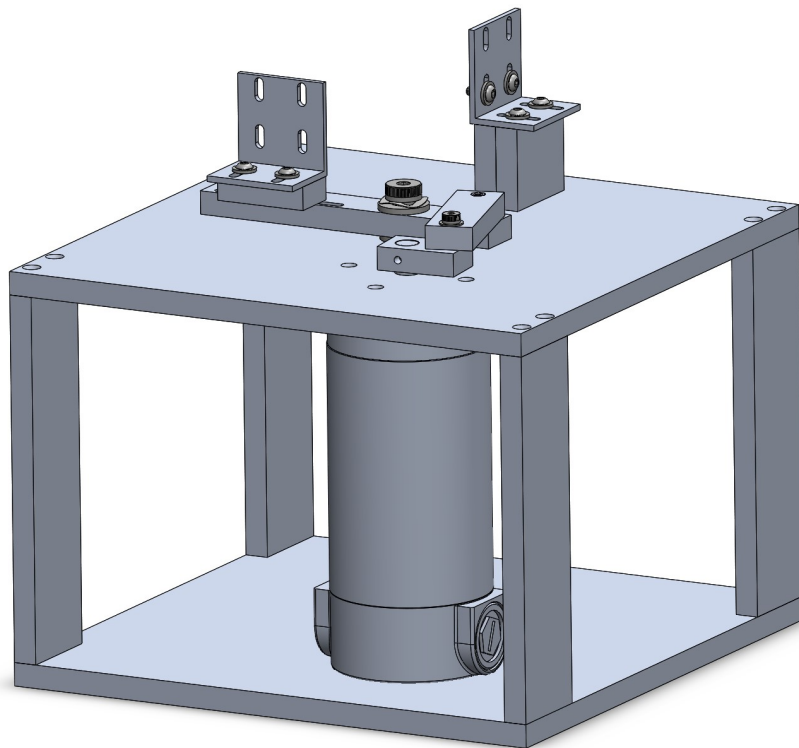


Figure 15. Isometric CAD View of Strap Cycle Machine.

C. Cycle Testing

Over the course of the planned mission life, it is estimated that the articulating thermal strap will undergo approximately 32,000 cycles over its entire rotational range. The goal for the risk reduction cycle testing was to determine what kind of mechanical degradation, if any, would be seen on the strap after cycling to at least four times mission life, or about 128,000 cycles.

The strap testing was conducted in two parts. The first part subjected just the thermal strap to > 130,000 cycles at a rate of approximately 1 cycle per second. Inspection of the strap following the test revealed no visible degradation of the strap, nor any particle generation.

A prototype SLI blanket was installed over the articulating thermal strap for the second part of the test. The SLI prototype blanket was made from 0.0005 inch thick VDA Kapton which had fiber reinforcement on its internal surface (Figure16). The second part of the test put another >130,000 cycles on the articulating thermal strap and SLI, for a total of > 260,000 cycles (8 times mission life) on the thermal strap and > 130,000 cycles (4 times mission life) on the SLI blanket. Inspection of the articulating strap and SLI following the second part of the test revealed no visible mechanical degradation of the thermal strap itself. Some minor permanent creasing was noted on the SLI blanket, however there was no visible particle accumulation.

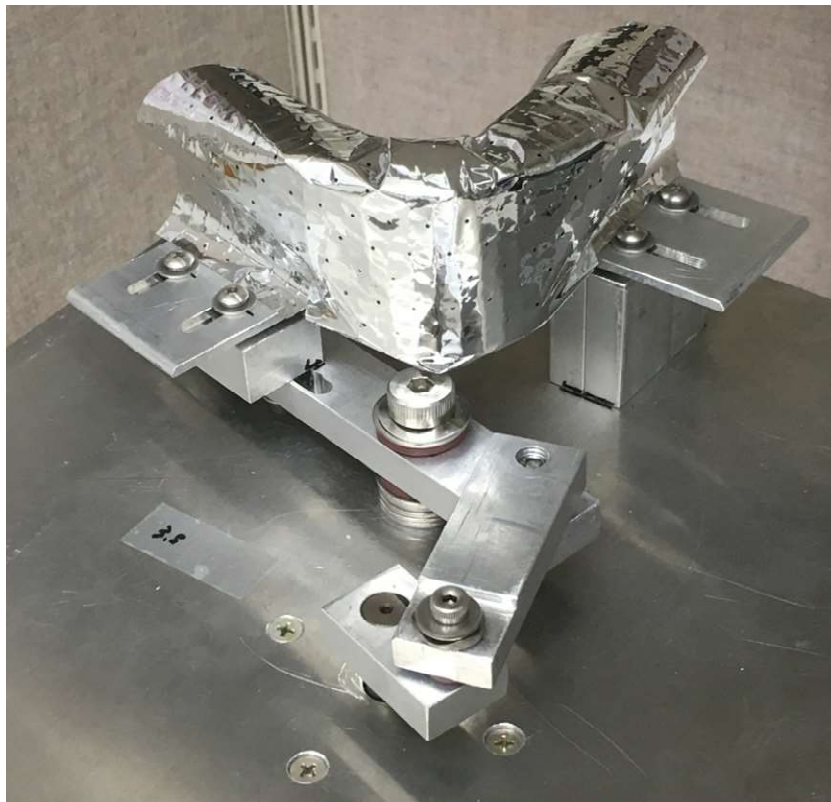


Figure 16. Thermal Strap with Prototype SLI Blanketing.

Additional life cycle testing of a flight configuration engineering model of the articulating thermal strap will be undertaken in the next phase of the MAIA project. This testing will run at the strap's expected operating temperatures and will measure variations in thermal conductance, as a function of articulation cycles.

VII. Analytical Modeling

Discussion in this section will provide an overview of the thermal analysis completed at the time of writing and will focus mainly on the thermal control of the FPM and cameras. Along with the orbital parameters mentioned earlier, the analysis assumed the unit dissipations in Table 1 along with the environmental constants provided in Table 2.

Table 2. Thermal Environmental Constant Assumptions.

Item	Minimum Value	Maximum Value
Solar Constant	1322 W/m ²	1414 W/m ²
Earth Shine	218 W/m ²	244 W/m ²
Albedo Fraction	0.24	0.35

Thermal modeling and analysis was performed using Thermal Desktop software². Overall views of the MAIA system level thermal model are shown in Figure 17. Note that the model includes notional blanketing that will cover the exposed harness and cables in the flight configuration. In addition, a representative bus was included in the model to simulate thermal loading from the yet-to-be-determined host.

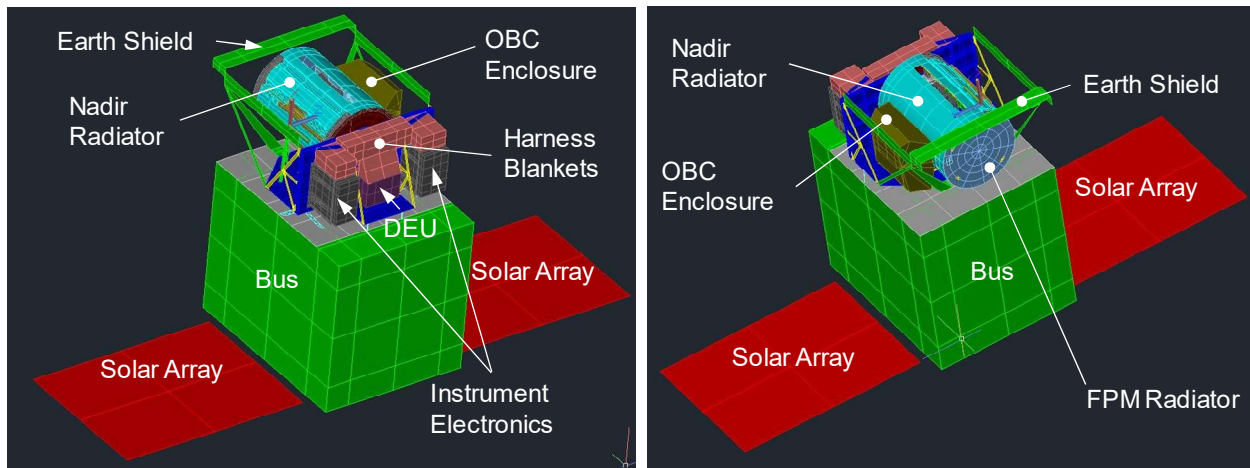


Figure 17. MAIA Thermal Model.

Figures 18 and 19 provide close-up views of the instrument thermal model showing the details of the FPM Radiator, the Nadir Radiator, the Earth Shield, the OBC enclosure and the gimbal support panel.

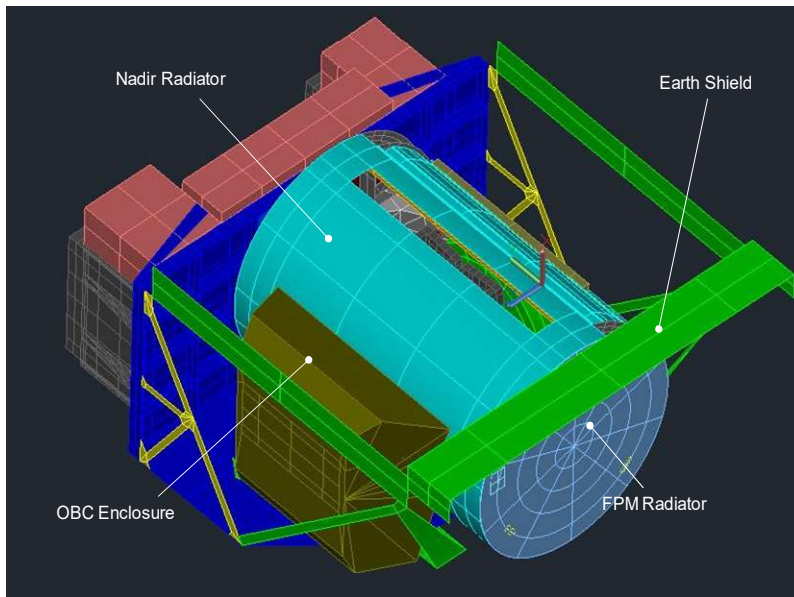


Figure 18. MAIA Thermal Model, External Detail 1.

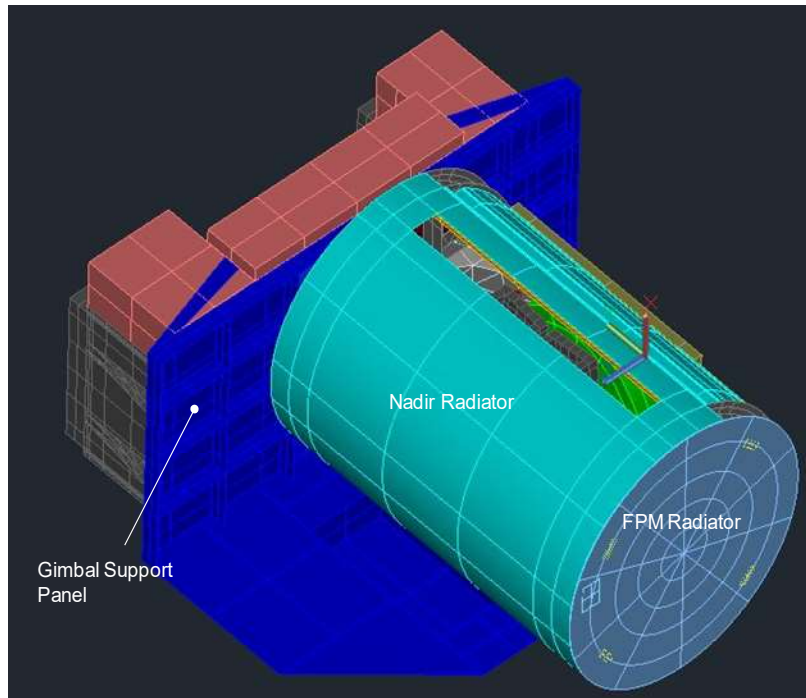


Figure 19. MAIA Thermal Model, External Detail 2.

Thermal modeling of instrument internal details are shown in Figures 20 and 21. Accurate representations of the cameras, camera electronics, FPMs, thermal straps and thermal links are included in the model. Notable assumptions for exposed surface optical properties are included in Table 3.

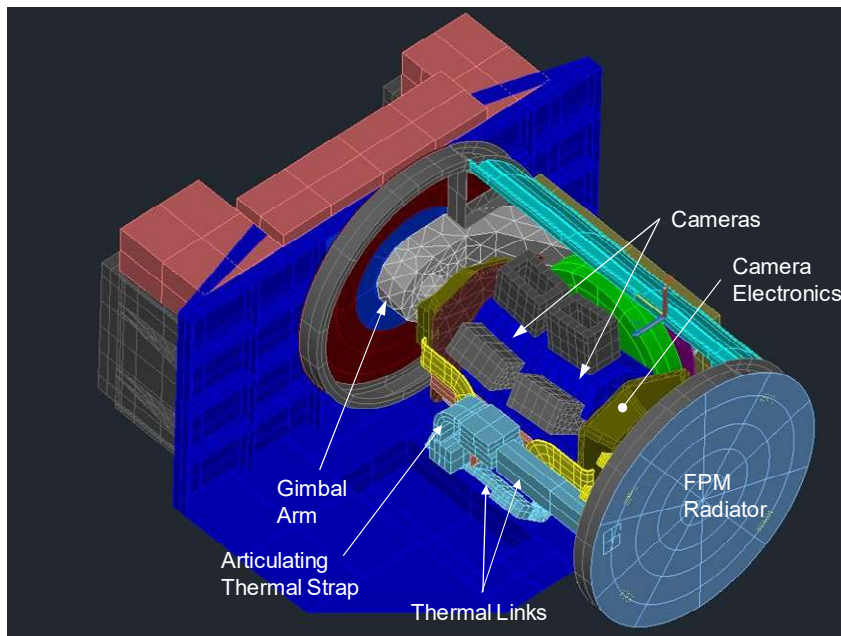


Figure 20. MAIA Thermal Model, Internal Detail 1.

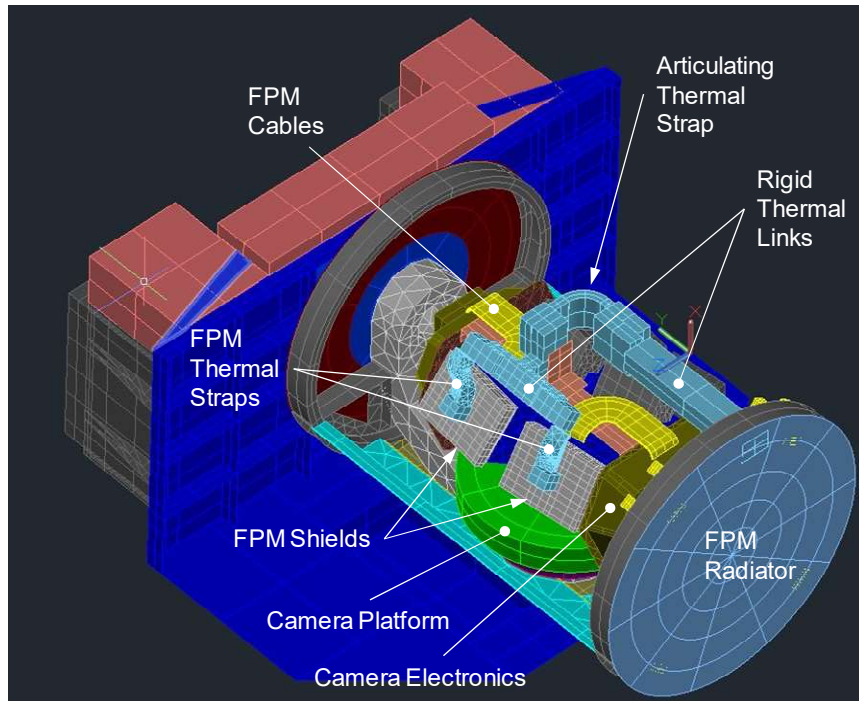


Figure 21. MAIA Thermal Model, Internal Detail 2.

Table 3. Notable Exposed Surface Thermal-Optical Property Assumptions.

Material Description	Solar Absorptivity (α)		Hemispherical Infrared Emissivity (ϵ)	
	BOL	EOL	BOL	EOL
Fused Silica (Quartz)	0.015	0.025	0.9	0.9
Vapor Deposited Aluminum Coated Kapton, Aluminum Side	0.12	0.12	0.03	0.03
Vapor Deposited Aluminum Coated Kapton, Kapton Side	0.49	0.7	0.83	0.83
Z306 Black Paint	0.95	0.93	0.87	0.87
S-13 White Paint	0.22	0.39	0.88	0.88

A large set of analysis cases, representing operating, non-operating and failure scenarios have been run with the thermal models to date. Descriptions of the bounding hot and cold operational cases is provided in Table 4.

Table 4. Bounding Operational Cases.

Case No	Description	Orbit	Beta (°)	Alt. (km)	Pointing	Solar Const. (W/m ²)	Albedo Fraction	Earth IR (W/m ²)	Optical Property Condition
C1	Bounding Cold Operational	Sun Sync	1	850	FPM Radiator Anti-Sun	1322	0.24	218	BOL
H1	Bounding Hot Operational	Sun Sync	55	600	FPM Radiator Anti-Sun	1414	0.35	244	EOL

Selected FPM and camera temperature results from the bounding hot and cold operational cases are included in Tables 5 and 6, along with operational temperature limits for each item. Table entries represent results from transient cases that had reached a dynamic steady state condition, where orbital minimums and maximums have stabilized. Columns labeled “Orbit Min Node” represent the coldest orbital temperature of the coldest node in the thermal model for the item of interest. Similarly columns labeled “Orbit Max Node” represent the hottest orbital temperature for the hottest node in the thermal model for the item of interest. Column’s labeled Max nodal variation represent the maximum orbital temperature variation for any single node within the thermal model for the item of interest.

Table 5. Selected Operational Temperature Predictions, Focal Plane Module.

Case No	Description	FPM Radiator		+Y FPM			-Y FPM			Operational Temperature Limits (K)	
		Orbit Min Node (K)	Orbit Max Node (K)	Orbit Min Node (K)	Orbit Max Node (K)	Max Nodal Variation (K)	Orbit Min Node (K)	Orbit Max Node (K)	Max Nodal Variation (K)	Min (K)	Max (K)
C1	Bounding Cold Operational	190.6	192.9	200.72	200.82	0.05	200.72	201.08	0.04	195	300
H1	Bounding Hot Operational	210.7	213.5	225.70	225.82	0.05	225.70	226.17	0.07		

Table 6. Selected Operational Temperature Predictions, Camera.

Case No	Description	Nadir Radiator		+Y Camera			-Y Camera			Operational Temperature Limits (K)	
		Orbit Min (K)	Orbit Max (K)	Orbit Min Node (K)	Orbit Max Node (K)	Max Nodal Variation (K)	Orbit Min Node (K)	Orbit Max Node (K)	Max Nodal Variation (K)	Min (K)	Max (K)
C1	Bounding Cold Operational	242.6	257.7	282.44	282.83	0.26	282.46	282.83	0.24	283	308
H1	Bounding Hot Operational	283.4	297.6	307.71	308.12	0.20	307.69	308.06	0.19	283	308

VIII. Hosted Payload Considerations

As mentioned previously, MAIA is a hosted instrument. It is likely that the MAIA project will have no knowledge of the spacecraft bus configuration, or adjacent payloads, until most of the detailed design is complete on the MAIA instrument. Clearly, influences from the spacecraft bus and adjacent payloads can have a significant impact on MAIA’s thermal performance. In an attempt to address this situation, a number of thermal requirements were included in the MAIA host interface requirements documentation. These requirements include items such as the thermal field-of-view (FOV) stay-out zones shown in Figure 22. Note that a 2π steradian unobstructed FOV for the FPM radiator is specified, as well as $\pm 85^\circ$ FOV stay-out zones for the Nadir Radiator about the X and Y instrument axes.

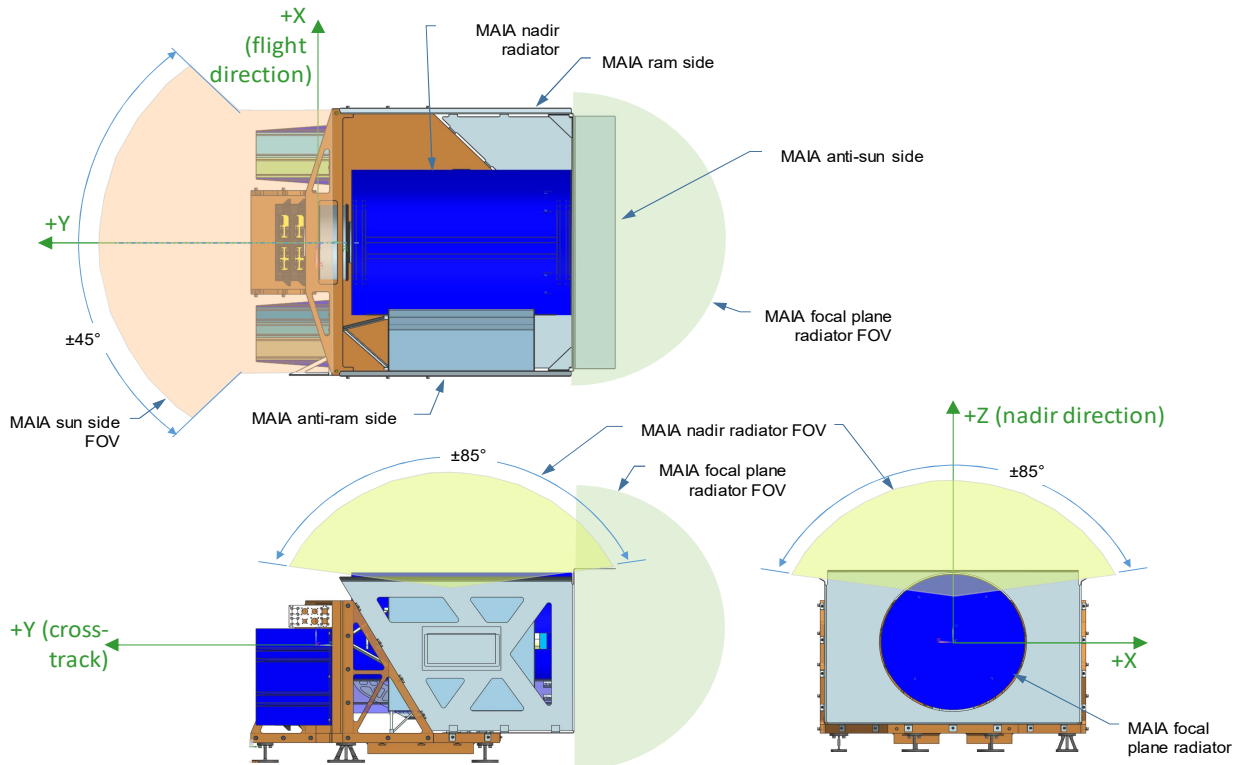


Figure 22. Thermal Field-of-View Stay-Out Zones Specified in MAIA Host Interface Requirements.

Additional host requirements specify the amount of infrared and solar spectrum radiation, incident upon the MAIA instrument, which is emitted from, or reflected by, adjacent payload and spacecraft bus surfaces.

Finally, requirements that dictate the allowable range of thermal conductance and heat flow at the MAIA instrument to bus interface were included in the host interface requirements documentation.

To help assess the potential influences of the spacecraft bus and adjacent payloads, bounding thermal analyses included blocking surfaces to simulate the worst case hosting environment (Figure 23).

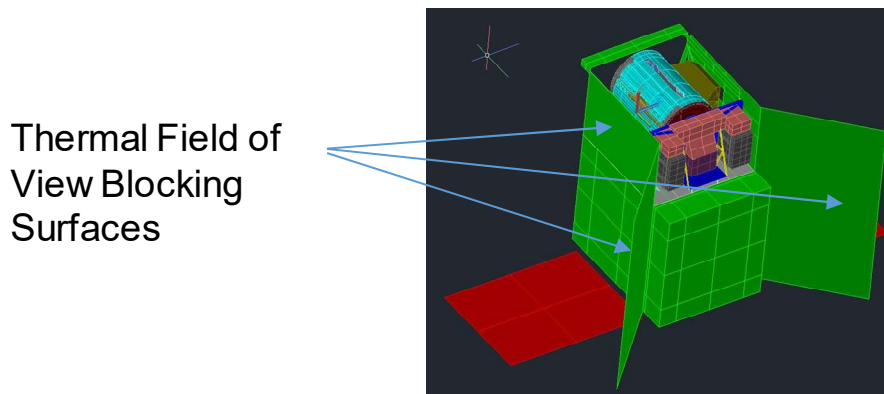


Figure 23. Thermal Blocking Surfaces Used to Simulate Adjacent Payloads.

IX. Conclusion

Thermal modeling to date indicates that the MAIA thermal control system will maintain operational temperatures within limits. Risk reduction testing demonstrates that the approach of using a rotationally articulating

thermal strap to transfer heat across the instruments rotating Pan axis is consistent with mission lifetime requirements.

Acknowledgments

The work described in this paper was carried out at the Jet Propulsion Laboratory, California Institute of Technology, under a contract with the National Aeronautics and Space Administration. In addition, the author would like to acknowledge the following people for their contributions to this effort: Dr. David Diner, Kevin Burke, Jose I. Rodriguez, Mason Mok, Andres Andrade, Mark D. Duran and Richard S. Frisbee.

References

¹Liu, Yang, and Diner, D. J. "Multi-Angle Imager for Aerosols: A Satellite Investigation to Benefit Public Health." *Public Health Reports* Vol. 132, No. 1, 2017, pp.14-17.

²C&R Technologies, 2501 Briarwood Dr., Boulder, CO 80305.